# Metasurfaces for Filter Miniaturization and Out-of-Band Rejection Improvement

Arash Arsanjani, *Graduate Student Member, IEEE*, Chad Bartlett, *Graduate Student Member, IEEE*, Luke Robins, Reinhard Teschl, *Member, IEEE*, Wolfgang Bösch, *Fellow, IEEE*, and Michael Höft, *Senior Member, IEEE*

***Abstract*— This work presents a novel implementation of metasurface filters with high performance and compact size for future space applications. A *K*-band fourth-order metasurface filter is proposed with a center frequency of 18.5 GHz and bandwidth of 400 MHz with an out-of-band rejection that is better than 30 dB over the range of 20–50 GHz. The proposed filter has a measured insertion loss of 1.47 dB and a quality factor of 670. The resonators implemented in this filter exhibit a miniaturization of 63% when compared to a conventional rectangular waveguide (RWG) resonator. The compact size and high-performance capabilities make the proposed filter an ideal solution for space applications.**

***Index Terms*— *K*-band, metasurfaces, microwave filters, miniaturization, slow-wave filter, spurious-mode rejection.**

## I. Introduction

FILTERS are an important building block of any telecommunication system. Most frequently, research on filter design for satellite telecommunication systems includes improvements in terms of quality factor, miniaturization, and out-of-band rejection. Each of these requirements is often addressed separately and can require tradeoffs in order to achieve specified goals. In regards to the quality factor, which determines the level of losses associated with a filter, many examples, such as [1] and [2] for *K*-band operation, and [3] and [4] for *W*-band operation, have been able to demonstrate compelling solutions using higher-order modes. In the effort to reduce the presence of spurious modes—which can often become too close to the passband—studies on the improvement of filter's out-of-band rejection by works such as [5], [6], [7], [8], and [9] provide effective solutions to suppress spurious modes. However, a method to achieve a well-balanced tradeoff, while effectively miniaturizing a given structure, is the use of metasurfaces inside the resonators [10], [11]. This method has been shown to achieve a miniaturization factor of up to 60% [10], [11].

Manuscript received 8 October 2022; revised 31 October 2022; accepted 2 November 2022. Date of publication 2 January 2023; date of current version 13 March 2023. This work was supported by the European Union's Horizon 2020 Research and Innovation Program under the Marie Skłodowska-Curie Grant 811232-H2020-MSCA-ITN-2018. *(Corresponding author: Arash Arsanjani.)*

Arash Arsanjani, Luke Robins, Reinhard Teschl, and Wolfgang Bösch are with the Institute of Microwave and Photonic Engineering, Graz University of Technology, 8010 Graz, Austria (e-mail: Arash.Arsanjani@tugraz.at).

Chad Bartlett and Michael Höft are with the Department of Electrical and Information Engineering, Kiel University, 24118 Kiel, Germany.

Color versions of one or more figures in this letter are available at https://doi.org/10.1109/LMWT.2022.3221467.

Digital Object Identifier 10.1109/LMWT.2022.3221467

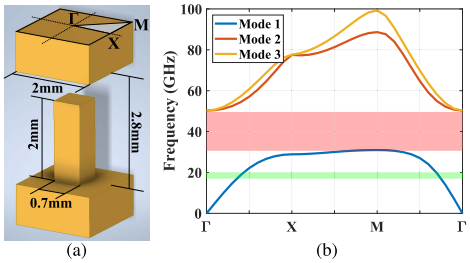


Fig. 1. Proposed unit cell for the filter design. (a) Structure and dimensions. (b) Band diagram that characterizes the electromagnetic properties of these unit cells over the irreducible Brillouin zone when forming an infinite periodic structure.

Metasurfaces are a branch of metamaterials, which focus on the properties and applications of 2-D periodic structures in a propagation medium [12]. These periodic structures have a frequency selective influence on the propagating waves, and if engineered properly, this feature can be used to improve the filter's out-of-band rejection response. In this manner, using periodic structures inside a propagating medium can increase the effective dielectric permittivity of the structure; therefore, miniaturization proportional to the effective dielectric permittivity of the metasurface is also expected. One benefit of these periodic structures is that they can be designed to exhibit a wide bandgap in the propagation constant, which can be used to reject certain spurious modes and create a wide out-of-band rejection response. The waffle-iron [13] working principle, for example, is based on the bandgap that the periodic structures create. However, the design procedure for these structures usually leads to bulky low-pass filters with wide passbands, which will reduce their cost-effectiveness despite their impressive out-of-band rejection level, while furthermore requiring precise alignment of the waffle-iron teeth during assembly.

This work demonstrates a novel solution for passband filters that are capable of obtaining wide out-of-band rejection characteristics with highly compact resonators. To achieve this, the demonstrated fourth-order *K*-band filter uses an offset fourth-order configuration for the rejection of the second and third resonating modes in combination with a metasurface unit cell, which is designed to suppress higher modes from 30 to 50 GHz. This work details the design of the unit cell, its integration into a filter structure, and presents the measured performance of the fabricated prototype. The fabricated filter achieves a quality factor of approximately 670 when operating at 18.5 GHz with a bandwidth of 400 MHz and an insertion loss of 1.47 dB at the measured center

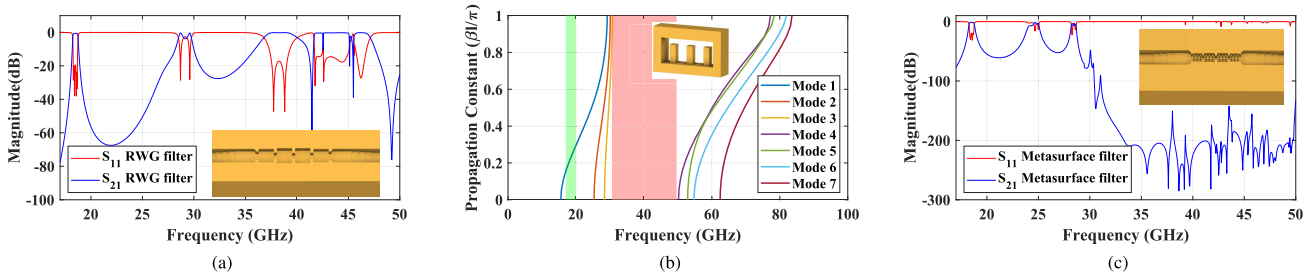


Fig. 2. Comparison of RWG filter and metasurface filter's frequency response. (a) Frequency response of a fourth-order RWG inline filter. (b) Propagation constant of the proposed metasurface transmission line. (c) Frequency response of the fourth-order metasurface inline filter.

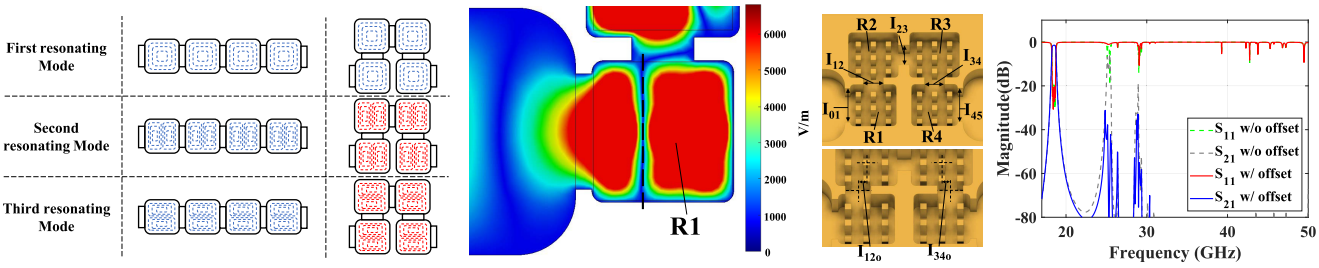


Fig. 3. Spurious mode rejection improvement based on filter's configuration adjustment. (a) Electrical field distribution of the first three resonating modes in inline and folded topology. (b) Electrical field distribution in the R1 resonator with loading effect. (c) Two configurations of the folded fourth-order filter (with and without the offset on the irises $I_{12}$ and $I_{34}$). (d) Frequency response of a fourth-order folded filter, with and without the offset.

frequency. The design of the filter exhibits a size reduction of approximately 63%, owing to an increase in the effective dielectric permittivity of the resonator, and this effect is a result of using metasurfaces.

## II. Metasurface Filter Design

The unit cell should be specifically designed to achieve the desired filter characteristics, that is, miniaturization and out-of-band rejection. The dimensions and spacing of the cells should be optimized to reject the required higher-order modes, while still achieving the required miniaturization effect. For this work, the chosen filter, a *K*-band filter with a center frequency of 18.5 GHz, a bandwidth of 400 MHz, and spurious mode rejection of better than 30 dB from 20 to 50 GHz, determines the requirements of the metasurface.

For this purpose, a simple bed-of-nails unit cell was designed, as shown in Fig. 1(a), with the first three propagating modes presented in Fig. 1(b). Fig. 1(b) highlights the first mode propagation with the desired bandwidth (the green zone from 17 to 20 GHz), which meets the requirement for a filter center frequency of 18.5 GHz. Furthermore, the bandgap region (red zone) can be exploited to block the higher-order spurious modes of the filter from 30 to 50 GHz.

An inline fourth-order rectangular waveguide (RWG) filter matching the passband specification previously discussed was designed for comparison. The frequency response, shown in Fig. 2(a), highlights the presence of strong spurious transmission between 25 and 50 GHz. Implementing the specified unit-cell pins into an RWG, as shown in Fig. 2(b), combines the cutoff frequency of the waveguide with the bandgap of the unit cell. Using the combination for resonators in a similar inline configuration leads to the response shown in Fig. 2(c). In this manner, the filter has no propagation from 30 to 50 GHz and exceeds the design specification in this range.

Despite the impressive rejection from 30 to 50 GHz, the elimination of the modes that are still propagating between 20 and 30 GHz is needed in order to meet the specified design requirements. In the ideal case, an alternative unit-cell geometry or type could have been selected to further shift the bandgap lower. This, however, would add complexity to the manufacturing process and limit the achievable accuracy. For this reason, a simple, repeatable unit-cell type was selected. Alternatively, negative couplings could have been used as well, but would have also increased the complexity of the structure.

The simplest approach in terms of complexity of implementation and occupied space, which was taken in this paper, was to manipulate the electromagnetic fields using the structural topology [14]. The second and third resonating modes are usually easier to deal with while trying to improve the rejection level. As an illustration, the electrical-field distribution of the waves is shown in Fig. 3(a). As can be seen, an approach to eliminate these modes is to use a folded configuration for the fourth-order filter structure.

Using a folded configuration, it can be seen from Fig. 3(d) that the modes between 20 and 30 GHz are decoupled better when compared to the typical inline configuration. However, the specific rejection level (below 30 dB) is still not met fully. This is due to the loading effect of the input and output on the first and fourth resonators, which changes the electrical-field distribution and increases the coupling through the irises $I_{12}$ and $I_{34}$. This effect in resonator R1 is shown in Fig. 3(b) for a better illustration. To further improve the rejection in this range, an offset is applied to the location of the aforementioned irises, which is shown in Fig. 3(c). In this manner, the final design reaches a rejection level of better than 30 dB for the second and third resonating modes, which adheres to the required filter specification.

The resonators used in the proposed filter, outlined in Fig. 4(a), achieved a high degree of miniaturization when

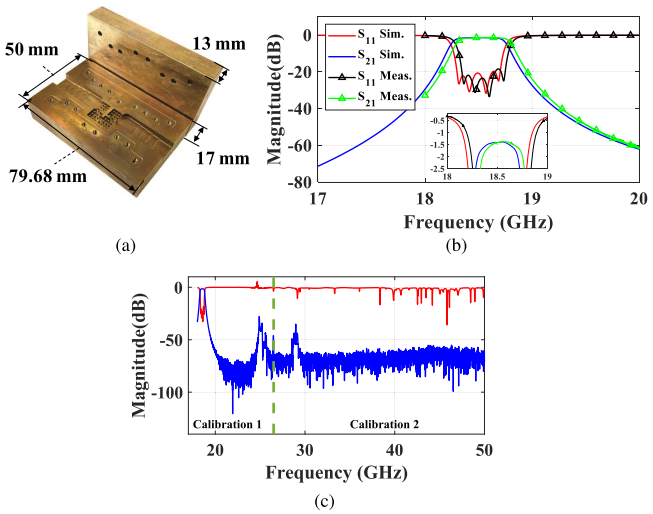


Fig. 4. Manufactured component and measurement results. (a) Finalized proposed filter with stepped impedance transformer for adaptation to a WR42 standard. (b) Passband frequency response, simulation versus measurement. (c) Wideband measurement of the filter.

compared to a conventional RWG resonator. For a direct comparison, the resonator R1 in the folded configuration has the dimensions of 6.63 × 6.63 × 2.8 mm. While resonator R1 in the conventional RWG filter, presented in Fig. 2(a), have the dimensions of 10.9 × 10.9 × 2.8 mm. The comparison of the two resonators shows that miniaturization of approximately 63% was achieved with the proposed structure. The folded configuration also adds a higher level of compactness in comparison to most filters with similar rejection characteristics, such as waffle iron [13], or corrugated filter topology [8].

The following instruction outlines the design procedure for the proposed filter.

1) Unit cells are designed for the specified bandgap and miniaturization.
2) The resonant frequency is adjusted by optimizing the resonator wall dimensions.
3) The bandgap is effectively designed to block modes higher than the second and third resonating modes. The second and third resonating modes' rejection can be improved by configuring the topology.

These three steps should be repeated until a filter with the widest out-of-band rejection and high miniaturization is realized with a medium to low level of sensitivity to fabrication tolerances.

## III. Fabrication and Measurement

The proposed filter was a fourth-order generalized Chebyshev filter with a passband of 400 MHz, return loss of 20 dB, and out-of-band rejection of better than 30 dB from 20 to 50 GHz. The fabricated component was milled using a brass alloy as depicted in Fig. 4(a), with the effective conductivity of approximately $1.15 \times 10^7$ S/m. The simulated and measured responses of the passband is shown in Fig. 4(b) where the measured insertion loss is better than 1.47 dB at the center frequency with a quality factor of approximately 670. An RWG using the same metal and having the same cavity height would have a quality factor of approximately 1400 while occupying the same space for a resonator, according to the simulations. A minor frequency shift of less than 50 MHz can be observed in the manufactured component, however this small deviation can be accounted for in future fabrication iterations.

TABLE I
Comparison to the State-of-the-Art

| Ref. | Freq. (GHz) | FBW | Insertion loss (dB) | Ratio* | Size |
|---|---|---|---|---|---|
| 2012 [8] | 11.7 | 17.1% | $\leq 0.5$ | 3.42 | $10.7\lambda_0 \times 0.74\lambda_0$ |
| 2019 [14] | 22.7 | 2.4% | 0.5 | 1.94 | $2.57\lambda_0 \times 1.52\lambda_0$ |
| 2021 [9] | 11.45 | 20% | 0.4 | 3.75 | $5.38\lambda_0 \times 0.72\lambda_0$ |
| 2021 [15] | 12 | 17.5% | $\leq 0.5$ | 1.33 | $0.3\lambda_0 \times 1.04\lambda_0$ |
| | 12.4 | 10.2% | $\leq 1$ | 1.23 | $0.22\lambda_0 \times 1.13\lambda_0$ |
| | 12.7 | 4.5% | $\leq 2$ | 1.18 | $0.18\lambda_0 \times 1.17\lambda_0$ |
| **This work** | 18.5 | 2.16% | 1.47 | 2.7 | $0.97\lambda_0 \times 0.85\lambda_0$ |

*Ratio is defined as the ratio of the upper stopband frequency to the center frequency.

The measurement of such a wide frequency range for the out-of-band rejection was challenging since the commercial waveguide adapters do not cover such a wide bandwidth. Therefore, the measurement was done in two stages. For the first, from 18 to 26.5 GHz, where a thru-reflect-line (TRL) calibration has been completed using the commercial waveguide adapters K281C from Keysight. For the second stage, the calibration from 26.5 to 50 GHz was done at the coaxial connector level and the measurement shown is with the consideration of adapters as a part of the component. The combined measurement is shown in Fig. 4(c). The spike seen in $S_{11}$ at approximately 25 GHz, which goes above 0 dB, is likely due to an error associated with the cables or adapters. However, from this procedure, it is shown that the out-of-band rejection level of the filter has been highly improved using a metasurface concept from 20 to 50 GHz while attaining a highly compact structure and excellent bandpass characteristics.

A comparison table of the proposed concept and the state-of-the-art has been provided for further elaboration in Table I. The comparison demonstrates that the proposed concept has shown a more efficient tradeoff between the miniaturization and performance of all the recent works. The work presented in [15] has the highest similarity to the proposed work and has achieved an impressive low profile. However, the proposed filter in this work provides a better filtering functionality with higher selectivity and better control of bandwidth.

## IV. Conclusion

A fourth-order folded metasurface filter has been proposed for *K*-band operation. Demonstration of the simulated and measured results shows an excellent out-of-band rejection performance. The proposed filter also exhibits a high degree of miniaturization which will make the proposed design a suitable solution for future space applications. Additionally, the high quality factor and low level of insertion loss, along with the ease of fabrication are the most important benefits of the proposed design.

## References

[1] B. Yassini, M. Yu, and B. Keats, "A *Ka*-band fully tunable cavity filter," *IEEE Trans. Microw. Theory Techn.*, vol. 60, no. 12, pp. 4002–4012, Dec. 2012, doi: 10.1109/TMTT.2012.2224367.

[2] S. Nam, B. Lee, C. Kwak, and J. Lee, "A new class of K-band high-Q frequency-tunable circular cavity filter," *IEEE Trans. Microw. Theory Techn.*, vol. 66, no. 3, pp. 1228–1237, Mar. 2018, doi: 10.1109/TMTT.2017.2778075.

[3] C. Bartlett, M. M. Gohari, O. Glubokov, J. Oberhammer, and M. Höft, "Compact triangular-cavity singlet-based filters in stackable multi-layer technologies," *IEEE Trans. THz Sci. Technol.*, vol. 12, no. 5, pp. 540–543, Sep. 2022.

[4] C. Bartlett and M. Höft, "Fully inline and symmetric dual-mode dual-band bandpass filters for millimetre-wave applications," in *IEEE MTT-S Int. Microw. Symp. Dig.*, Nov. 2021, pp. 323–325.

[5] O. A. Peverini et al., "Integration of an H-plane bend, a twist, and a filter in Ku/K-band through additive manufacturing," *IEEE Trans. Microw. Theory Techn.*, vol. 66, no. 5, pp. 2210–2219, May 2018, doi: 10.1109/TMTT.2018.2809505.

[6] A. R. Azad and A. Mohan, "Substrate integrated waveguide dual-band and wide-stopband bandpass filters," *IEEE Microw. Wireless Compon. Lett.*, vol. 28, no. 8, pp. 660–662, Aug. 2018, doi: 10.1109/LMWC.2018.2844103.

[7] L. Ma, J. Li, Y. Zhou, X. Sun, and H. Zhu, "Substrate integrated waveguide filter with higher-order modes suppression," in *Proc. Int. Conf. Microw. Millim. Wave Technol. (ICMMT)*, May 2018, pp. 1–3, doi: 10.1109/ICMMT.2018.8563942.

[8] I. Arregui et al., "High-power low-pass harmonic waveguide filter with $TE_{n0}$-mode suppression," *IEEE Microw. Wireless Compon. Lett.*, vol. 22, no. 7, pp. 339–341, Jul. 2012.

[9] M. Yang et al., "Design of wide stopband for waveguide low-pass filter based on circuit and field combined analysis," *IEEE Microw. Wireless Compon. Lett.*, vol. 31, no. 11, pp. 1199–1202, Nov. 2021, doi: 10.1109/LMWC.2021.3087703.

[10] A. Arsanjani, L. Robins, B. Meier, J. Petrusa, R. Teschl, and W. Bosch, "Additive manufacturing of a 4th-order K-band semi-planar slow-wave filter," in *IEEE MTT-S Int. Microw. Symp. Dig.*, Nov. 2021, pp. 332–334, doi: 10.1109/IMFW49589.2021.9642380.

[11] A. Arsanjani, H. S. Farahani, B. Rezaee, R. Teschl, and W. Bosch, "A compact slow-wave filter with double-sided selectivity and wide out-of-band rejection," in *Proc. IEEE Asia–Pacific Microw. Conf. (APMC)*, Nov. 2021, pp. 256–258, doi: 10.1109/APMC52720.2021.9661651.

[12] F. Mesa, G. Valerio, R. Rodriguez-Berral, and O. Quevedo-Teruel, "Simulation-assisted efficient computation of the dispersion diagram of periodic structures: A comprehensive overview with applications to filters, leaky-wave antennas and metasurfaces," *IEEE Antennas Propag. Mag.*, vol. 63, no. 5, pp. 33–45, Oct. 2021, doi: 10.1109/MAP.2020.3003210.

[13] F. Teberio et al., "Design procedure for new compact waffle-iron filters with transmission zeros," *IEEE Trans. Microw. Theory Techn.*, vol. 66, no. 12, pp. 5614–5624, Dec. 2018.

[14] Q. Wu, F. Zhu, Y. Yang, and X. Shi, "An effective approach to suppressing the spurious mode in rectangular waveguide filters," *IEEE Microw. Wireless Compon. Lett.*, vol. 29, no. 11, pp. 703–705, Nov. 2019.

[15] M. K. Moghaddam and R. Fleury, "Miniaturized metamaterial filters compatible with standard waveguide technology," in *Proc. 15th Int. Congr. Artif. Mater. Novel Wave Phenomena (Metamaterials)*, Sep. 2021, pp. 197–199.